J Mater Sci (2008) 43:635–640
DOI 10.1007/s10853-007-2154-0

On the crystallization kinetics and micro-structural transformations of $Fe_{40}Ni_{38}B_{18}Mo_4$ alloys

Thomas Hysen · Thomas Senoy · R. V. Ramanujan · M. R. Anantharaman

Received: 9 August 2006 / Accepted: 10 September 2007 / Published online: 17 October 2007

Abstract Activation energy for crystallization (E_c) is a pertinent parameter that decides the application potential of many metallic glasses and is proportional to the crystallization temperature. Higher crystallization temperatures are desirable for soft magnetic applications, while lower values for data storage purposes. In this investigation, from the heating rate dependence of peak crystallization temperature T_p, the E_c values have been evaluated by three different methods for metglas 2826 MB ($Fe_{40}Ni_{38}B_{18}Mo_4$) accurately. The E_c values are correlated with the morphological changes, and the structural evolution associated with annealing temperatures is discussed.

Introduction

Recently there is renewed interest in amorphous alloys due to the superlative properties exhibited by their nanocrystalline counterparts. The first report of nanocrystallization in amorphous alloys by Yozhizawa, Oguma and Yamauchi on Fe–Si–B–Nb–Cu in 1988 [1] triggered similar studies on several other transition metal based metallic glasses. The extreme magnetic softness exhibited by these alloys can be attributed to the averaging of anisotropies over grains and the counterpoise between exchange correlation length and grain size. They exhibit ferromagnetism characterized by high saturation magnetization, vanishing magnetic anisotropy, negligible magnetostriction and large magnetic permeability [2–5]. They also exhibit interesting magneto-acoustic and magneto-optical properties, which can be utilized for many applications.

$Fe_{40}Ni_{38}B_{18}Mo_4$ is one such material widely used for sensor and soft magnetic applications [6]. Its softness after devitrification can be ascribed to its biphasic nature consisting of a nanocrystalline Fe–Ni–Mo phase embedded in the remaining boron rich amorphous phase [7]. It also shows a typical two stage crystallization similar to most Fe based metallic glasses. The two phases are reported to have Curie temperatures 760 K and 485 K respectively, and have different contributions to the total saturation magnetizations. The Curie temperature 626 K and low saturation magnetostriction 12 ppm accounts for the superior soft magnetic properties exhibited by the bulk material. The material can be tailored by field annealing for superior soft magnetic properties such as coercivity H_c = 7 mOe, retentivity M_r = 7.5 kG and a dc relative permeability of about 45,000 [8]. These superlative properties have been exploited for various technological applications namely sensors, actuators, shielding, high frequency transformer cores, magneto-optic sensors and magnetic recording.

Thermal processes are known to be important in inducing crystallization in metallic glasses. There have been diverse views about the crystallization stages of metglas. In the present work, a detailed study of the crystallization kinetics of amorphous $Fe_{40}Ni_{38}B_{18}Mo_4$ alloy has been made using Differential Scanning Calorimetry (DSC)

T. Hysen
Department of Physics, Christian College, Angadical, Chengannur, Kerala 689 122, India
e-mail: hysenthomas@gmail.com

T. Hysen · T. Senoy · M. R. Anantharaman (✉)
Department of Physics, Cochin University of Science & Technology, Cochin, Kerala 682 022, India
e-mail: mra@cusat.ac.in
e-mail: hysenthomas@gmail.com

R. V. Ramanujan
School of Materials Science and Engineering, Nanyang Technological University, Singapore 639 798, Singapore

and X-ray diffraction (XRD). The thermal stability and crystallization kinetics of the system is also discussed.

The sudden quenching associated with the production processes forces metallic glasses to relax from a higher stable enthalpy state to a lower meta-stable enthalpy state. This type of thermal relaxation will be more profound near the glass transition temperatures T_g. The crystallization kinetics of amorphous alloys can be studied using different characterization tools. Utilizing the thermo dynamical evolution of the system, two techniques namely isothermal and non-isothermal colorimetric studies can be used. In the former, the heat evolved during the isothermal crystallization process is recorded as a function of time, when the sample is raised to a temperature above T_p. In the latter, temperature of the sample is increased at a fixed rate b to a value above T_p and the heat evolved is recorded as a function of temperature [9]. We have employed non-isothermal calorimetric studies at different heating rates for evaluating the kinetic parameters.

Crystallization proceeds through nucleation, growth of crystalline phases and Ostwald ripening and thus is primarily governed by the thermodynamics of the system and the diffusivities of constituent atoms. These three stages of crystallization have characteristic activation energies and without loosing generality, one can combine all these processes into a single activation energy [10]. The approximation is justified by the reasoning that for most of the materials the three stages have overlapping energy curves.

Upon heating to higher temperatures from room temperature, metallic glasses exhibits different stages of crystallization characterized by the appearance of different crystalline phases. Antonione et al. [11] was the first to report the crystallization kinetics of metglas. Using non-isothermal calorimetric studies they reported activation energies of $\approx$3.067 eV/atom and $\approx$3.46 eV/atom respectively for the two phases. However, Majumdar and Nigam observed three stage crystallization in the material [12]. Cubrera et al. carried out a quantitative investigation on the crystallization kinetics and estimated the activation energies of the two phases using both non-isothermal and isothermal methods employing DSC, DTA and resistivity measurements [13]. The respective values obtained were $\approx$2.984 eV/atom and $\approx$3.678 eV/atom from non-isothermal and $\approx$2.984 eV/atom and $\approx$4.673 eV/atom from isothermal methods for the first and second phases respectively. Using non-isothermal techniques Nicolai found five step crystallization in the sample and the activation energies were reported to be $\approx$2.92 ev, and $\approx$3.85 ev for the FeNi and cubic boride phases [14]. Recently, Du et al. reported the activation energies $\approx$4.24 eV/atom and $\approx$5.13 eV/atom using non-isothermal DSC and resistivity measurements [15]. The above discussion suggests that reports on the crystallization kinetics of metglas are rather scanty, and there exists diverse opinions about the E_c values for the nucleation and phase separation. In the present work, we report the crystallization kinetics of metglas 2826 MB employing DSC, XRD and analysis methods like Kissinger [16], and Moyniham [17] and Marseglia [18] techniques. A precise knowledge about the kinetics of crystallization is extremely important to determine the activation energy for crystal growth. The intention of present study is to apply calorimetric methods to establish the mechanism of crystallization and to evaluate the activation energy of crystallization.

Experimental

High purity alloy ribbons with composition $Fe_{40}Ni_{38}B_{18}Mo_4$ prepared by melt quenching technique were subjected to X-ray diffraction to confirm their amorphous nature. The ribbons were 20 μm in thickness and 25 mm in width. They were subjected to non-isothermal DSC studies for heating rates 5, 10, 20 and 25 K/min. The activation energies were estimated employing the Kissinger, Moynihan and Marseliga techniques. On the bases of the results of DSC studies, the samples were subjected to thermal annealing at a high vacuum of $\approx 10^{-6}$ Torr. The sample temperatures are heated to the annealing temperature at a heating rate of 5 K/min and maintained at that temperature for one hour and subsequently cooled with the same ramp rate. The spectra of the metglas samples, pristine and annealed were recorded with Rigaku D-max-C X-ray diffractometer using CuK_α radiation (λ = 1.5405 Å). The d values were calculated using the equation $d = \left(\frac{\lambda}{2\sin\theta}\right)$ and the planes are indexed using JCPDS database. The average particle size is determined from the measured width of their respective diffraction curves using Debye Scherer formula $D = \left(\frac{0.9\lambda}{\beta\cos\theta}\right)$, β is the full width at half maximum [FWHM].

Results and discussion

Crystallization studies

The non-isothermal DSC studies conducted on the ribbons for various heating rates clearly indicate a two-step devitrification process (Fig. 1). The small dip found in the DSC exotherms just before the first crystallization step is due to the structural relaxation occurring in the alloy. This indicates that the structure may have started to relax far below the crystallization temperature. Glassy state is characterized by large viscosity and hence the relaxation kinetics is relatively sluggish leaving little room for local

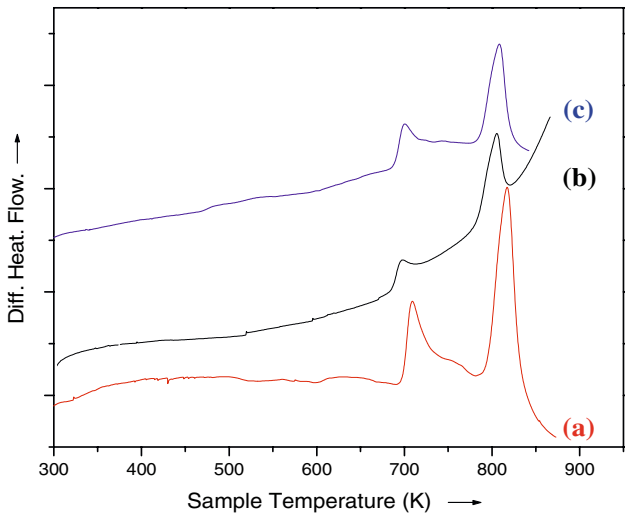

Fig. 1 DSC thermogram of metglas ribbons for heating rates (**a**) 20 K/min (**b**) 10 K/min (**c**) 5 K/min

atomic rearrangements. This type of thermal relaxation is prominent near the glass transition temperature, which manifests as an endothermic peak in the DSC due to change in specific heat. However, if the relaxation is fast, such an endothermic peak emerges as a small dip due to a fast change in total heat content. This can be utilized for studying the thermodynamic behaviour of the sample. The heating rate dependence of the glass transition temperature in metallic glasses is usually interpreted by invoking the physics of thermal relaxation phenomenon. During this process, the free volume is annealed out. Two main exothermic peaks were found in the DSC, which can be attributed to the two stages of crystallization corresponding to the two phases. The first peak rises sharply, which indicates spontaneous nucleation and grain growth, which suggests that the delay between nucleation and grain growth is very small. This can be ascribed to the relative ease of expulsion of highly diffusive boron from the vicinity of FeNiMo clusters. The slow growth of second phase implies slow nucleation and growth of the second phase at the expense of the first phase. The first exotherm, which is asymmetric attributes to the devitrification process resulting in a homogeneously dispersed Fe–Ni–Mo nano phase embedded in the residual boron rich amorphous matrix. Further, it is evident that the first crystallization step extends up to the initial stage of the second crystallization with progressive grain growth of the initially nucleated crystallites. The initial crystalline phase is responsible for the superlative magnetic properties exhibited by metglas [19]. The second DSC exotherm corresponds to crystallization of the residual amorphous phase and the precipitation of $FeNiMo_{23}B_6$ [19]. The crystallization temperatures associated with the two phases are 699 K and 809 K correspondingly for a heating rate of 15 K/min. The enthalpy change associated with crystallization, which corresponds to the maximum energy associated with the phase transformations were estimated to be 13.9 J/g and 51.1 J/g respectively. The lower enthalpy of formation of the first phase is indicative of easy nucleation of the first phase at lower annealing temperatures. The higher enthalpy of the second phase implies higher annealing temperatures and higher thermal energies for nucleation and growth.

Structural analysis

The X-ray diffraction pattern of the unannealed metglas ribbons is shown in Figs. 2a and 3a. The pristine films show broad diffraction peaks, which indicate their amorphous nature and the fine dispersion of Fe and Ni in the sample. However, the diffraction patterns of the annealed ribbons (Figs. 2b, 3b, c) clearly indicate crystallization in the sample with thermal treatments. The ribbons annealed at 773 K in vacuum possess heterogeneous microstructure consisting of FeNiMo and $FeNiMo_{23}B_6$. At temperatures intermediate between the crystallization temperatures of the two phases, FeNi crystallites tends to grow to micrometric dimensions. Figure 3b and c shows the XRD spectrum of pristine and ribbons annealed at 623 and 773 K. There is progressive grain growth of FeNiMo phase with increase in annealing temperatures. Above 350 K, $FeNiMo_{23}B_6$ phase starts to appear whose presence is reported to have been deleterious to the soft magnetic properties [20]. The intensity of boride phase increases

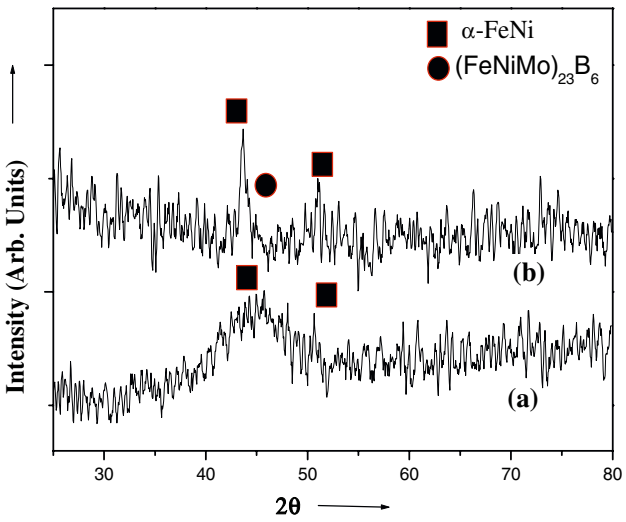

Fig. 2 XRD spectrum of metglas ribbons (**a**) unannealed (**b**) annealed at 773 K.

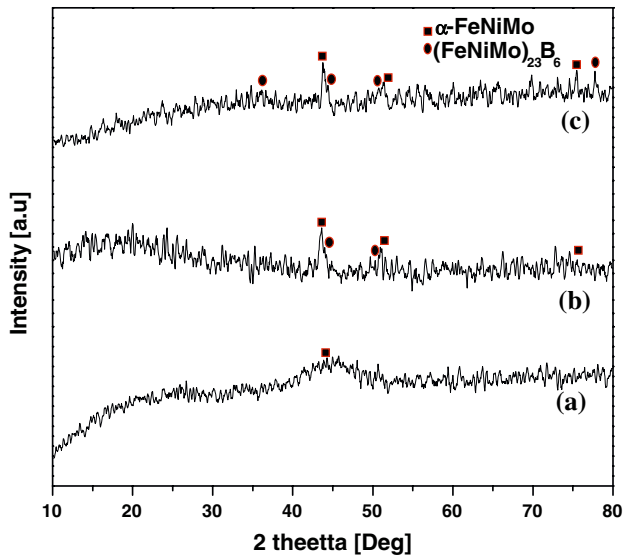

Fig. 3 XRD spectrum of metglas ribbons annealed at various temperatures. (**a**) unannealed ribbon (**b**) annealed at 623 K (**c**) annealed at 773 K

with annealing temperature at the expense of the FeNiMo phase, while the FeNiMo crystallite size increases.

Estimation of activation energy

Any crystal growth process can be characterized by two types of activation energies, the activation energy for nucleation and activation energy for growth. Usually, the two energy barriers are considered to be condensed into a single energy barrier referred to as the activation energy for growth E_c, since usually these two processes are separated by very low barriers. The activation energies are usually evaluated from DSC thermograms for various heating rates employing different models. When the temperature is raised to 740 K, the α-FeNiMo phase increases and new phases of $FeNiMo_{23}B_6$ appear, while the amorphous phase almost vanishes [20]. Our results are consistent with the investigations of Du et al. [7]. The experimental data on crystallization has been analysed using Kissinger [16], Moynihan [17] and Marseliga [18] techniques for the estimation of activation energy [21].

Kissinger model

During an isothermal transformation subjected to an instantaneous isobaric change, the crystallization process is usually represented by the Avrami's [22] equation

$$x(t) = 1 - e^{-(Kt^n)} \tag{1}$$

where K is the rate constant and n is the order parameter, which incorporates the dimensionality of crystal growth. The rate constant obeys an Arrhenius type relation

$$K = K_o e^{\left(-\frac{E_c}{k_B T}\right)} \tag{2}$$

According to Kissinger, Eq. 1 can be approximated as

$$\frac{dx}{dt} = (1-x)nK^n t^{n-1} \tag{3}$$

Expressing t in terms of x from Eq. 1 the rate of crystallization becomes

$$\frac{dx}{dt} = AnK(1-x) \tag{4}$$

where

$$A = [-\ln(1-x)]^{\frac{n-1}{n}} \tag{5}$$

However, in non-isothermal crystallization, the heating rate is assumed to be a constant and the relation between the sample temperature T and heating rate b can be written as

$$T = T_i + bt \tag{6}$$

where T_i is the initial temperature.

The time derivative of K can be evaluated using Eqs. 2 and 6 as

$$\frac{dK}{dt} = \left(\frac{dK}{dT}\right)\left(\frac{dT}{dt}\right) = \left(\frac{bE_c}{RT^2}\right)K \tag{7}$$

Using Eqs. 4 and 7, Kissinger showed that

$$\ln\left(\frac{b}{T_p^2}\right) = -\frac{E_c}{RT_p} + C \tag{8}$$

where C is a characteristic constant of crystallization [23].

In this method, the activation energy is determined by plotting $\ln\left(\frac{b}{T_p^2}\right)$ versus $\frac{1000}{T_p}$, the slope of the straight line fit gives $-\frac{E_c}{1000R}$ from which the E_c values were evaluated. Figures 4 and 5 show the Kissinger plot for Fe–Ni–Mo–B system for the two phases.

Moynihan model

This is another relation, which connects the shifts in T_p values of DSC with the heating rate. An instantaneous isobaric change in temperature of a glassy system causes the total heat content $H(T, t)$ to settle down isothermally to

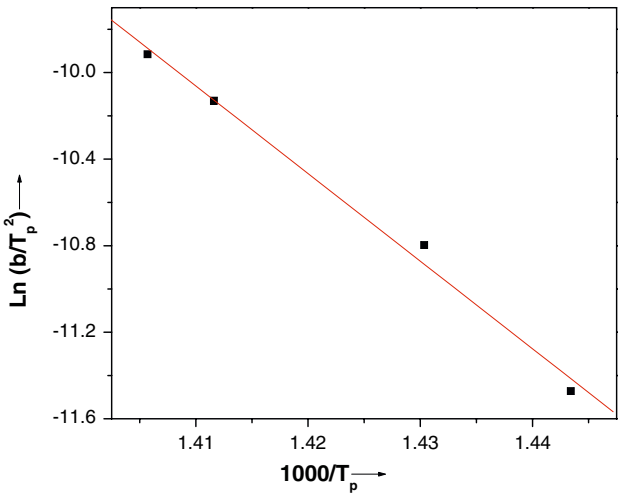

Fig. 4 Kissinger plot corresponding to the first peak in the DSC exotherm

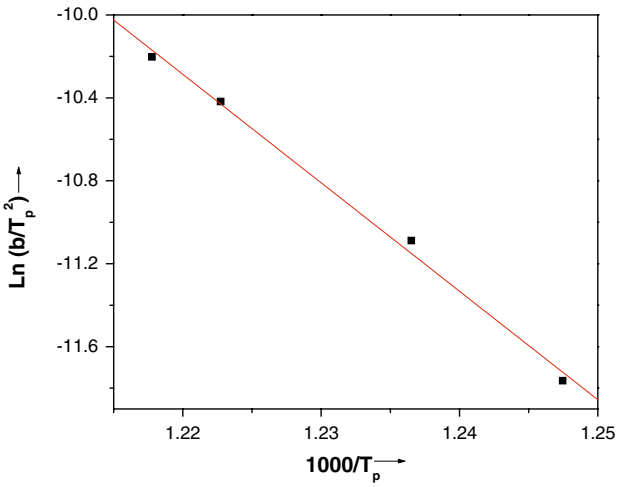

Fig. 5 Kissinger plot corresponding to the second peak in the DSC exotherm

a new equilibrium value $H(T)$. The relaxation can be mathematically expressed as,

$$\left(\frac{\delta H}{\delta t}\right)_T = -\frac{(H - H_e)}{t} \tag{8}$$

here t is the structural relaxation time, which is dependant on temperature and is given by

$$t = t_o e^{\left(\frac{-\Delta E_r}{k_B T}\right)} e^{[-r(H-H_e)]} \tag{10}$$

where t_o and r are constants and E_r is the activation energy of relaxation time. Using the above equations, it can be shown [17, 24] that;

$$\frac{d(\ln b)}{d\left(\frac{1}{T_p}\right)} = \frac{\Delta E_c}{k_b} \tag{11}$$

k_b is the Boltzman's constant. Figures 6 and 7 show the plots of ln b with $\frac{1000}{T_p}$ for Fe–Ni–Mo–B for the two crystalline phases. The activation energies are calculated from the slopes of the straight line fits.

Marseliga model

In 1980, Marseglia had suggested a theory for evaluating activation energies from DSC thermograms [18, 25]. Accordingly,

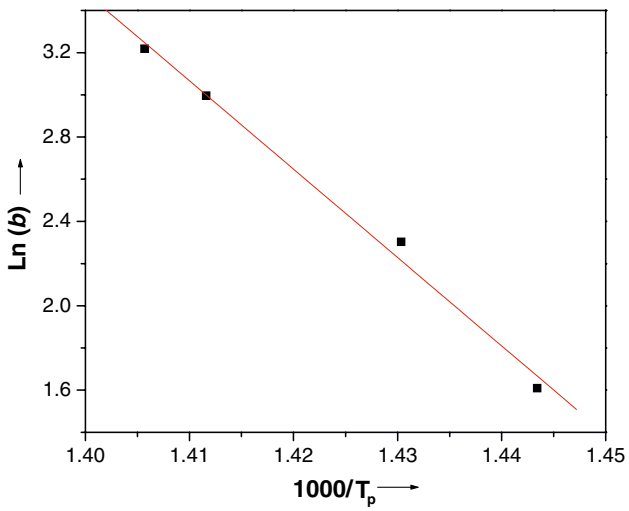

Fig. 6 Moynihan plot corresponding to the first peak in the DSC exotherm

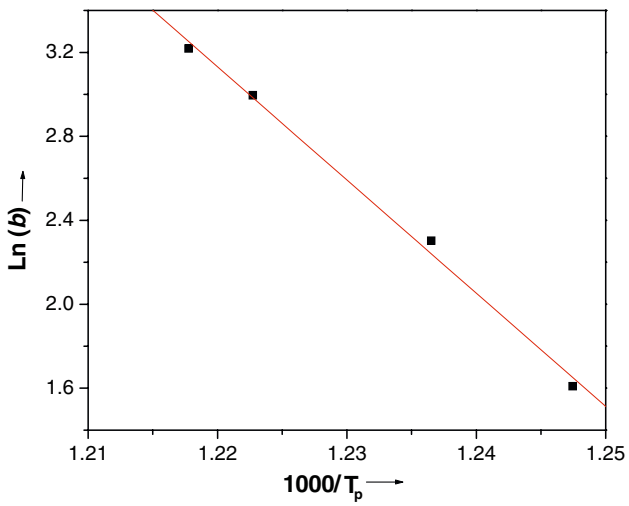

Fig. 7 Moynihan plot corresponding to the second peak in the DSC exotherm

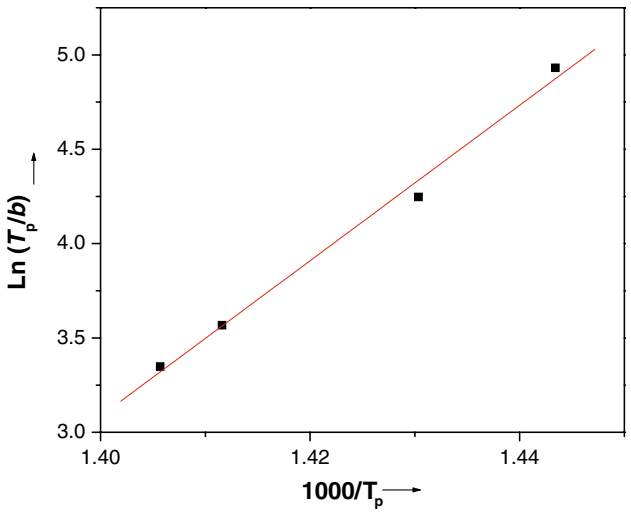

Fig. 8 Marseliga plot corresponding to the first peak in the DSC exotherm

$$\ln\left(\frac{T_p}{b}\right) = \frac{E_c}{kT_p} + C, \tag{12}$$

where C is a characteristic constant, and Figs. 8, 9 shows the Marseliga plots for the two crystalline phases from which the E_c values were evaluated.

The activation energies calculated using the above three techniques and the respective mean values for the two phases were tabulated in Table 1.

Conclusions

The heating rate dependence b of T_p is used to evaluate the activation energy of crystallization for the Fe–Ni–Mo and boride phases. The activation energies estimated using Kissinger, Moynihan and Marseglia methods agree fairly well. The E_c values for crystallization for the Fe–Ni–Mo phase is found to be 3.55 ± 0.22 eV/atom. The comparatively higher values of activation energy is suggestive of the higher thermal stability of metglas. The E_c value for the second phase is found to be 4.58 ± 0.21 eV/atom. This value being higher indicates that massive elements like molybdenum, which are active elements during the second crystallization process, can raise the activation energy of crystallization in metallic glasses. From the XRD spectrum, it is evident that the first phase is Fe–Ni–Mo and the second phase is $FeNiMo_{23}B_6$.

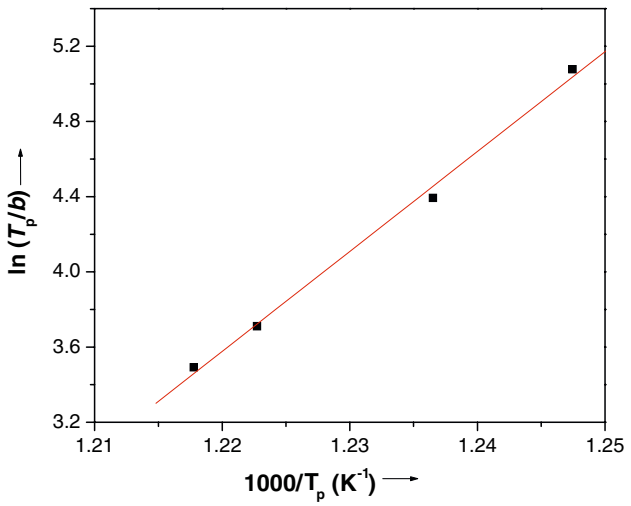

Fig. 9 Marseliga plot corresponding to the second peak in the DSC exotherm

Table 1 Activation energies calculated using three different models

Theory	E_c values for I Peak eV/atom	E_c values for II Peak eV/atom
Kissinger	3.49 ± 0.22	4.51 ± 0.21
Moynihan	3.61 ± 0.22	4.65 ± 0.21
Marseliga	3.55 ± 0.22	4.58 ± 0.21
Mean	3.55 ± 0.22	4.58 ± 0.21

References

1. Yoshizawa Y, Oguma S, Yamauchi K (1988) J Appl Phys 64:6044
2. Gleiter H (1989) Prog Mater Sci 33:223
3. Arcas J, Vasquez M, Hernando A, Gomez-Polo C (1997) Sens Actuators A59:101
4. Chiriac H, Hristoforou E, Neagu M, Darie I, Nagacevschi V (1997) Mater Sci Eng A 226:1093
5. Shirae S (1979) J Appl Phys 50:7618
6. Grimes CA, Kouzoudis D (2000) Sens Actuators 84:205
7. Du SW, Ramanujan RV (2005) J Meta Nano Mater 23:207
8. Hesagava R, Narasimhan MC, Decristofara N (1978) J Appl Phys 49:1712
9. Saxena M, Bhatnagar PK (2003) Bull Mater Sci 26:547
10. Ram S (2004) Curr Sci 86:832
11. Antonione C, Battezzati L, Lucci A, Riontino G, Venturelo G (1978) Scripta Met 12:1011
12. Majumdar AK, Nigam AK (1980) J Appl Phys 51:4218
13. Cumbrera FL, Miranda H, Conde A, Marquez R, Vigier P (1982) J Mater Sci 17:2677, doi: 10.1007/BF00543904
14. Nicolai HP, Kopmann G, Frommeyer G (1981) Z Metallkd 72:558
15. Du SW, Ramanujan RV (2004) Mater Sci Eng A 375:1040
16. Kissinger HE (1957) Anal Chem 29:1702
17. Moynihan CT, Easteal AJ, Wilder J, Tucker J (1974) J Phys Chem 78:267
18. Marseglia EA (1980) J Non-Cryst Solids 41:31
19. Raja VS, Kishore, Ranganathan S (1987) Bull Mater Sci 9:207
20. Hysen T, Deepa S, Saravanan S, Ramanujan RV, Avasthi DK, Joy PA, Kulkarni SD, Anantharaman MR (2006) J Phys D: Appl Phys 39:1993
21. Manish Saxena (2004) Bull Mater Sci 27:543
22. Avrami M (1939) J Chem Phys 7:1103; (1940) 8:212; (1941) 9:177
23. Kissinger HE (1956) J Res Nat Bur Stand 57:217
24. Mahadevan S, Giridhar A, Singh AK (1986) J Non-Cryst Solids 88:11
25. Atmani H (1988) Mater Chem Phys 19:255